Assessment of Sea Ice Simulations in the CMIP5 Models

Qi Shu[1, 2], Zhenya Song[1, 2], Fangli Qiao[1, 2]

1 {First Institute of Oceanography, State Oceanic Administration, Qingdao 266061}

2 {Key Lab of Marine Science and Numerical Modeling, SOA, Qingdao 266061}

Correspondence to: Fangli Qiao (qiaofl@fio.org.cn)

Abstract

The historical simulations of sea ice during 1979 to 2005 by the Coupled Model Intercomparison Project Phase 5 (CMIP5) are compared with satellite observations, Global Ice-Ocean Modeling and Assimilation System (GIOMAS) output data and Pan-Arctic Ice Ocean Modeling and Assimilation System (PIOMAS) output data in this study. Forty-nine models, almost all of the CMIP5 climate models and Earth System Models with historical simulation, are used. For the Antarctic, multi-model ensemble mean (MME) results can give good climatology of sea ice extent (SIE), but the linear trend is incorrect. The linear trend of satellite-observed Antarctic SIE is $1.29(\pm 0.57)\times 10^5$ km^2 $decade^{-1}$; only about 1/7 CMIP5 models show increasing trends, and the linear trend of CMIP5 MME is negative with the value of $-3.36(\pm 0.15)\times 10^5$ km^2 $decade^{-1}$. For the Arctic, both climatology and linear trend are better reproduced. Sea ice volume (SIV) is also evaluated in this study, and this is a first attempt to evaluate the SIV in all CMIP5 models. Compared with the GIOMAS and PIOMAS data, the SIV values in both Antarctic and Arctic are too small, especially for the Antarctic in spring and winter. The GIOMAS Antarctic SIV in September is 19.1×10^3 km^3, while the corresponding Antarctic SIV of CMIP5 MME is 13.0×10^3 km^3, almost 32% less. The Arctic SIV of CMIP5 in April is 27.1×10^3 km^3, which is

also less than that from PIOMAS SIV (29.5×10^3 km^3). This means that the sea ice thickness simulated in CMIP5 is too thin although the SIE is fairly well simulated.

1. Introduction

The Coupled Model Intercomparison Project Phase 5 (CMIP5) provides a very useful platform for studying climate change. Simulations and projections by more than 60 state-of-the-art climate models and Earth System Models are archived under CMIP5. Assessment of the performance of CMIP5 outputs is necessary for scientists to decide which model outputs to use in their research and for model-developers to improve their models. Here, we focus on the assessment of sea ice simulations under CMIP5 historical experiment. The CMIP5 data portal contains sea ice outputs from 49 coupled models. Many of these CMIP5 sea ice simulations have been evaluated and several valuable studies have been published.

For the Antarctic, the main problem of the CMIP5 models is their inability to reproduce the observed slight increase of sea ice extent (SIE). Turner et al. (2013) first assessed CMIP5 Antarctic SIE simulations using 18 models, and summarized that the majority of these models have too little SIE at the minimum sea ice period of February, and the mean of these 18 models' SIE shows a decreasing trend over 1979-2005, opposite to the satellite observation that exhibits a slight increasing trend. Polvani et al. (2013) used four CMIP5 models to study the cause of observed Antarctic SIE increasing trend under the conditions of increasing greenhouse gases and stratospheric ozone depletion. They concluded that it is difficult to attribute the observed trend in total Antarctic sea ice to anthropogenic forcing. Zunz et al. (2013) suggested that the model Antarctic sea ice internal variability is an important metric to evaluate the observed positive SIE trend. Using simulations from 25 CMIP5 models, Mahlstein et al. (2013) pointed that internal sea ice variability is large in the Antarctic region and that both the observed and simulated trends may represent natural variation along with external forcing.

For the Arctic, CMIP5 models offer much better simulations. Stroeve et al. (2012) evaluated CMIP5 Arctic SIE trends using 20 CMIP5 models. They found that the seasonal cycle of SIE was well represented, and that the simulated SIE decreasing trend was more consistent with the observations over the satellite era than that of CMIP3 models but still smaller than the observed. They also noted the spread in projected SIE through the 21^{st} century from CMIP5 models is similar to that from CMIP3 models. Massonnet et al. (2012) examined 29 CMIP5 models, and provided several important metrics to constrain the projections of summer Arctic sea ice projection. Liu et al. (2013) also pointed out that CMIP5 projections have large inter-model spread, but they also found that they could reproduce agreed Arctic ice-free time by reducing the large spread using two different approaches with 30 CMIP5 models.

Most evaluations of CMIP5 sea ice simulation in these studies are based only on some of CMIP5 models' outputs with some metrics because other CMIP5 model outputs were not yet submitted. By now, all the CMIP5 participants have finished their model runs and submitted their model outputs. So, here we will evaluate all CMIP5 sea ice simulations with more metrics in both Antarctic and Arctic, in an attempt to provide the community a useful reference. Generally speaking, our study show that the performance of Arctic sea ice simulation is better than that of Antarctic sea ice simulation, sea ice extent simulation is better than sea ice volume simulation, and mean state simulation is better than long-term trend simulation. If we want to get the similar result with all CMIP5 sea ice simulations, the number of CMIP5 model we used during analysis should be more than 22.

The rest of the paper is structured as follows. Section 2 presents sea ice data and analysis methodology used in this study. Model assessment is given in section 3. Conclusions and discussion are provided in section 4.

2. Data and Methodology

Sea ice simulations of CMIP5 historical runs from 49 CMIP5 coupled models are now available. Monthly sea ice concentration (SIC) and sea ice thickness from these models are used in this study. These outputs are published by the Earth System Grid Federation (ESGF) (http://pcmdi9.llnl.gov/esgf-web-fe/) by each institute that is responsible for its model. Although there are several ensemble realizations of each CMIP5 model, the standard deviation between different ensemble realizations of each model is small (Turner et al., 2013; Table 1). We also plot the spatial patterns of SIC in February (Supplementary Fig. 1) and September (Supplementary Fig. 2) from different ensemble realizations from GISS-E2-R which has 15 ensemble realizations and have more ensemble realizations than most CMIP5 models. We can see that the standard deviation between different ensemble realizations from the same model is comparable. So, here we only choose the first realization of each model for the analysis. CMIP5 historical runs cover the period from 1850 to 2005, but the continuous sea ice satellite record only started in 1979; so the period of 1979-2005 is chosen for the following analysis. Monthly satellite-observed SIC is used in this study, which is based on the National Aeronautics and Space Administration (NASA) team algorithm (Cavalieri et al., 1996) provided by the National Snow and Ice Data Centre (NSIDC) (http://nsidc.org/data/seaice/). Satellite observed sea ice extent used here is also from NSIDC (ftp://sidads.colorado.edu/DATASETS/NOAA/G02135/). Sea ice volume (SIV) is an important index for assessment of sea ice simulation although direct observations of SIV are very limited. SIV in the Antarctic used here is from the Global Ice-Ocean Modeling and Assimilation System (GIOMAS) (http://psc.apl.washington.edu/zhang/Global_seaice/index.html). SIV in the Arctic is from Pan-Arctic Ice Ocean Modeling and Assimilation System (PIOMAS) (http://psc.apl.washington.edu/wordpress/research/projects/arctic-sea-ice-volume-anomaly/). Note that SIV data from GIOMAS and PIOMAS are not observations but model simulations with data assimilation. Stroeve et al. (2014) compared observed sea ice thickness data in the Arctic with that of PIOMAS, and concluded that

PIOMAS provides useful estimates of Arctic sea ice thickness and SIV, and can be used to access the CMIP5 models' performances. But there are not enough observations to validate GIOMAS sea ice thickness in the Antarctic. The climatology and linear trends of CMIP5 simulated SIE, SIC and SIV are compared with satellite observations and GIOMAS and PIOMAS data. CMIP5 simulated SIE is computed as the total area of all grid cells where SIC exceeds 15%. SIV is computed as the sum of the product of SIC, the area of grid cell and sea ice thickness of each grid cell. All gridded SIC and sea ice thickness are re-gridded onto 1.0° longitude by 1.0° latitude grids before the analysis is performed. In this study, spring is from March to May for the Arctic, and from September to November for the Antarctic. Summer, autumn and winter are defined accordingly.

3. Results

We select several metrics to assess the sea ice simulations in CMIP5 models. Mean state, seasonal cycle, the model internal variability, linear trends and simulated errors are used. For the Arctic sea ice, model mean state and seasonal cycle are important to Arctic sea ice projection (Massonnet et al., 2012). For the Antarctic sea ice, the model internal variability is an important metric to evaluate the observed positive SIE trend (Zunz et al., 2013). Annual mean SIE, SIE amplitude, standard deviation of detrended SIE anomaly (SIE variability), SIE linear trend and CMIP5 simulated SIE root mean square (RMS) error are shown in Table 1 and Table 2. The same metrics for SIV are also shown in Table 1 and Table 2. Each CMIP5 model simulated SIC and sea ice thickness are given in the Supplementary. Detailed analyses for Antarctic and Arctic are as follows.

3.1 Assessment of Antarctic sea ice simulations

CMIP5 multi-model ensemble mean (MME) Antarctic climatological SIE compares well with the satellite-observed SIE, but the inter-model spread is large (Fig. 1a and Table 1). Satellite observations show that the Antarctic SIE has the minimum value of 3.0 million km^2 in February and the maximum value of 18.7 million km^2 in September, and the annual mean SIE is 11.94 million km^2. CMIP5 MME SIE has the minimum and maximum values of 3.3 and 18.7 million km^2, and annual mean SIE of 11.50 million km^2, respectively. The seasonal cycle of observed SIE is well represented by the MME SIE of the 49 CMIP5 coupled models. Satellite observed monthly SIE amplitude is 15.70 million km^2, and CMIP5 MME value is 15.46 million km^2. The simulated SIE errors are very small for each month. The simulated SIE errors are smaller than 15% of the observations, except for March and April SIE values, which are a little less than 85% of the observations. One standard deviation of CMIP5 simulations, which is greater than 15% of the observations (Fig. 1a), show that CMIP5 coupled models have large spread each month in terms of Antarctic SIE. Table 1 also shows that CMIP5 models have large spread. BNU-ESM has the largest annual mean and amplitude of SIE with the values of 20.60 and 23.46 million km^2, and MIROC5 has the smallest annual mean and amplitude of SIE with the values of 3.23 and 6.62 million km^2 (highligthed in Table 1 with bold font), respectively. BNU-ESM simulated February SIE is even larger than MIROC5 simulated September SIE. Large SIE spread and small MME SIE errors indicate that we should use as many models as we can when using CMIP5 outputs.

CMIP5 model simulated and satellite observed SICs in February and September during 1979-2005 are shown in Supplementary Figures 3 and 4. In February most models have too less SIC compared with satellite observed, especially in the Bellingshausen Sea and the Amundsen Sea. More than half of CMIP5 models have no sea ice in the Bellingshausen Sea and the Amundsen Sea. CNRM-CM5, GFDL-CM2p1, GFDL-CM3, GFDL-ESM2G, GFDL-ESM2M, IPSL-CM5B-LR and MIROC5 almost have no sea ice in February in the Antarctic. But ACCESS1.3,

BNU-ESM, CCSM4, CESM1-BGC, CESM1-FASTCHEM, CSIRO-Mk3.6, FGOALS-g2, FIO-ESM and NorESM1-ME have more sea ice than satellite observations. Although CMIP5 simulated MME SIE fits the observations well, MME spatial map of SIC fits the observations not so well. MME SICs in the Weddell Sea, the Bellingshausen Sea and the Amundsen Sea are too little. In September, most CMIP5 models have better performance than that in February, and MME SIC also has better spatial pattern.

Figures 1b and 2 show that linear trends of CMIP5 MME Antarctic SIE do not agree with the satellite observations. Many studies showed that Antarctic SIE has an increasing trend since the end of 1970s (Cavalieri et al., 1997; Zwally et al., 2002; Cavalieri et al., 2003; Turner et al., 2009). Satellite-observed Antarctic SIE has a small increasing linear trend with the rate of $1.29(\pm 0.57)\times 10^5$ km^2 $decade^{-1}$ during 1979-2005, while CMIP5-simulated linear trend is $-3.36(\pm 0.15)\times 10^5$ km^2 $decade^{-1}$ (Fig. 1b). Only eight out of 49 CMIP5 models have increasing linear trends as the observations (highligthed in Table 1 with bold font). They are BCC-CSM1.1, CMCC-CESM, CNRM-CM5-2, GISS-E2-R-CC, IPSL-CM5A-MR, IPSL-CM5B-LR, MPI-ESM-MR and MRI-CGCM3. This supports the conclusion by Polvani et al. (2013) that it is difficult to attribute the observed Antarctic SIE trends to anthropogenic forcing. From Table 1 we can see that several models (highligthed in Table 1 with bold font) such as BCC-CSM1.1, BCC-CSM1-1-M, CanESM2, CMCC-CESM, CNRM-CM5-2 and GISS-E2-R have large internal variabilities, and these models always have large linear trends. This mean that the satellite observed positive SIE trend may represent natural variation along with external forcing (Mahlstein et al., 2013). Figure 2 shows that the monthly and seasonal trends of CMIP5-simulated Antarctic SIE also do not agree with the observations. Observed Antarctic SIE shows increasing trends in each month and each season, and the largest trend is in March and the autumn season. CMIP5 MME SIE, however, has decreasing trends in each month and each season, and the largest trend is in February and the summer season.

The trends of observed Antarctic SIC have large spatial differences (Fig. 3), but the simulated Antarctic SIC trends are almost decreasing everywhere (Fig. 4). Figure 3 shows that decreasing SIC is mainly in the Antarctic Peninsula, which is one of the three high-latitude areas showing rapid regional warming over the last 50 years (Vaughan et al., 2003). SIC also decreases in the Bellingshausen Sea and the Amundsen Sea in summer and autumn. The increasing SIC is mainly in the Ross Sea all year round and in the Weddell Sea in summer and autumn. Figure 4 clearly shows that CMIP5 MME SIC has decreasing trend everywhere except in the coast of the Amundsen Sea and in part of the Ross Sea in spring and winter.

SIV depends on both sea ice coverage and sea ice thickness. SIV is more directly tied to climate forcing than SIE. So, SIV is an important climate indicator in climate study. The observed sea ice thickness records are mainly from submarine, aircraft and satellite. But the observations are not continuously spatially or temporally over a long period (Stroeve et al., 2014). For the Antarctic, the observed sea ice thickness data are more limited. A climatological $2.5^{\circ} \times 5.0^{\circ}$ gridded Antarctic sea ice thickness map was provided until 2008 (Worby et al., 2008). Recently, there are several studies using satellite observations of sea ice thickness (Kurtz and Markus, 2012; Xie et al., 2013). These observations provide modelers with useful validation of their models. But, these data are not easily used to long-term simulation validations by now because these data are not too long enough. Here, we use GIOMAS data, which is from a global ice-ocean model (Zhang and Rothrock, 2003) with data assimilation capability. What we should keep in mind is that GIOMAS sea ice thickness is not from observations and may also have large uncertainty. CMIP5-simulated and GIOMAS Antarctic sea ice thicknesses during 1979-2005 are shown in Supplementary Figure 5. GIOMAS outputs show that thick sea ice is mainly in the coasts of the Weddell Sea, the Bellingshausen Sea and the Amundsen Sea. CMIP5 MME sea ice thickness can give similar spatial patterns, but most of CMIP5 MME sea ice thickness is thinner than GIOMAS sea ice thickness. The spatial pattern for each CMIP5 model has large difference. BCC-CSM1.1, CESM1-CAM5-1-FV2, CMCC-CM, and CMCC-CMS fit

GIOMAS sea ice thickness well. Several CMIP5 models such as CCSM4, CESM1-BGC, CESM1-FASTCHEM, FGOALS-g2 and FIO-ESM have too thick sea ice near the coasts of the Antarctic.

CMIP5 SIV simulations have more problems than the SIE simulations. The main problems of CMIP5 Antarctic SIV simulations include too big SIV in summer, too small SIV in winter, too large model spread, and wrong linear trend compared with the GIOMAS data (Fig. 5). The annual mean SIV from GIOMAS is 11.02×10^3 km^3, but CMIP5 MME SIV is only 7.73×10^3 km^3 (Table 1). In February, Antarctic SIV from GIOMAS is 1.9×10^3 km^3, while the CMIP5 MME is 2.7×10^3 km^3. In September, GIOMAS SIV is 19.1×10^3 km^3, while CMIP5 MME is only 13.0×10^3 km^3, almost 32% less than the GIOMAS. We can also see from Figure 5a that the model spread of Antarctic SIV in CMIP5 is very large. The one standard deviation is greater than 15% of the GIOMAS data in every month. We checked the correlation between SIE RMS error and SIV RMS error, and we can find that the models with small SIE RMS errors always have small SIV RMS errors (Table 1). It means that for the Antarctic models with a more realistic SIE mean state may result in a convergence of estimates of SIV. Figure 5b shows that GIOMAS SIV has an increasing trend of $0.45(\pm0.09)\times10^3$ km^3 $decade^{-1}$, while CMIP5 MME SIV has a decreasing trend of $-0.36(\pm0.01)\times10^3$ km^3 $decade^{-1}$. If we check each CMIP5 model separately, we will also find only eight out of the 49 CMIP5 models have increasing SIV trend that is consistent with the GIOMAS. They are BCC-CSM1.1, CMCC-CESM, CNRM-CM5-2, IPSL-CM5A-MR, IPSL-CM5B-LR, MPI-ESM-MR, MPI-ESM-P and MRI-CGCM3 (highligthed in Table 1 with bold font).

3.2 Assessment of Arctic sea ice simulations

CMIP5 shows a quite good annual cycle of Arctic SIE, but the model error in winter is larger than that in summer and model spread is large (Fig. 6a). Arctic SIE reaches the maximum value of 15.7 million km^2 in March, and reaches the minimum value of

6.9 million km^2 in September, and the annual mean value is 12.02 million km^2. The MME climatological SIE compares well with the satellite-observed SIE. CMIP5 MME SIE reaches the maximum value of 17.2 million km^2, and reaches the minimum value of 6.8 million km^2, and the annual mean value is 12.81 million km^2. The modeled error is less than 15% of the observations in every month. CMIP5 MME SIE is bigger than the satellite observation in spring, and the modeled error is quite small at other times. The model spread is large, with one standard deviation greater than 15% of the observed SIE in every month (Fig. 6a). CSIRO-MK3.6, GFDL-ESM2G, GISS-E2-R-CC and MRI-CGCM3 have large annual mean SIE with the values larger than 15 million square kilometers (highligthed in Table 2 with bold font). CSIRO-MK3.6 has more sea ice in the Barents Sea in summer (Supplementary Fig. 6). GFDL-ESM2G, GISS-E2-R-CC and MRI-CGCM3 have more sea ice in winter (Supplementary Fig. 7). MIROC4h, MIROC-ESM, MIROC-ESM-CHEM and MPI-ESM-P have small annual mean SIE with the values less than 11 million square kilometers (highligthed in Table 1 with bold font). Arctic SIE amplitudes from CMIP5 models also have large spread. GISS-E2-R-CC has the largest amplitude with the value of 16.73 million km^2, and FGOAL-g2 has the smallest amplitude with the value of only 3.35 million km^2 (highligthed in Table 2 with bold font). Compared with Antarctic, CMIP5 simulated Arctic SIE variability has small spread (Column c in Table 2).

CMIP5 MME SIE shows a decreasing trend that is consistent with the satellite observation, though the decreasing rate is a little smaller than that of the observation (Figs. 6b and 7). The satellite-observed SIE linear trend over the period of 1979-2005 is $-4.35(\pm 0.41)\times 10^5$ km^2 $decade^{-1}$, while CMIP5 MME SIE linear trend is only $-3.71(\pm 0.19)\times 10^5$ km^2 $decade^{-1}$. BCC-CSM1.1 has the largest trend of $-8.79(\pm 0.97)$ $\times 10^5$ km^2 $decade^{-1}$. Thirty-one out of the 49 CMIP5 models have smaller decreasing rate than the observation, and NorESM1-ME has the smallest trend of $-0.21(\pm 0.43)$ $\times 10^5$ km^2 $decade^{-1}$. Both observed and CMIP5-simulated SIE in autumn has the largest decreasing trend. CMIP5-simulated difference of SIE decreasing trend between summer and autumn is, however, larger than that of the observations. The main reason is CMIP5-simulated SIE has small reduction in summer, especially in July (Fig. 7). Satellite-observed SIE decreasing rate is 5.22% per decade in July, while the CMIP5-simulated decreasing rate is 3.54% per decade. The largest decreasing rate is in September; the observed trend is -8.61% per decade and the simulated trend is -8.46% per decade.

Figure 8 and 9 show that the spatial patterns of CMIP5-simulated SIC reduction rate are consistent with the observations from 1979 to 2005, but the decreasing rates are smaller than the observed. In spring and winter, the observed decreasing SIC is mainly in the Okhotsk Sea, Baffin Bay, Greenland Sea and Barents Sea; CMIP5-simulated decreasing SIC is also in these regions. In summer and autumn, the main decreasing SIC is in the Chukchi Sea, Barents Sea and Kara Sea (Figs. 8 and 9), and CMIP5 MME SIC has similar characteristics. However, CMIP5 simulations have larger trends in the central Arctic Ocean.

Compared with PIOMAS sea ice thickness, the main problem of CMIP5 simulations is too little Arctic SIV all year round and too large model spread (Fig. 10). In spring, the Arctic has the largest SIV. Long-term mean PIOMAS SIV is maximum in April with 29.5×10^3 km^3, and the corresponding CMIP5 MME is 27.1×10^3 km^3. Long-term mean PIOMAS SIV is minimum in September with 13.3×10^3 km^3, and the corresponding CMIP5 MME is 9.6×10^3 km^3. Amplitude of SIV from PIOMAS is 16.17×10^3 km^3, and CMIP5 MME can give good amplitude of SIV with 17.50×10^3 km^3. CMIP5 SIV model spread is also very large: one standard deviation for each month is greater than 15% of GIOMAS SIV. CanESM2 has the smallest SIV of 9.97×10^3 km^3, and CMCC-CM has the largest SIV of 33.01×10^3 km^3. Supplementary Figure 8 shows that BCC-CSM1-1-M, CanCM4, CanESM2, GFDL-CM2p1, GISS-E2-H, GISS-E2-H-CC, GISS-E2-R, GISS-E2-R-CC, MIROC4h, MIROC-ESM, and MIROC-ESM-CHEM simulated sea ice thickness is significantly undervalued. Sea ice thickness in CESM1-WACCM, CMCC-CESM, CMCC-CM, FGOALS-g2, IPSL-CM5B-LR, NorESM1-M, NorESM1-ME is significantly overvalued. Based on

PIOMAS, the linear trend of Arctic SIV during 1979-2005 is -2.14(±0.14)×10^3 km^3 $decade^{-1}$. CMIP5 MME trend has the same sign but smaller value, at -1.45(±0.05)× 10^3 km^3 $decade^{-1}$. Unlike most of CMIP5 models, CESM1-WACCM SIV has a slight positive trend during 1979-2005. The reason may be CESM1-WACCM SIV has large variability (2.07×10^3 km^3), and its internal variability is not in phase with the natural observed variability.

4. Conclusions and discussion

The first ensemble realizations of the 49 CMIP5 historical simulations are evaluated, in terms of the performance of sea ice. Our results show that the Arctic sea ice simulations are better than the Antarctic sea ice simulations, and SIE simulations are better than SIV simulations. CMIP5 MME SIV is too less in winter and spring because the sea ice thickness in CMIP5 models is too thin in winter and spring compared with the GIOMAS and PIOMAS data. In the Antarctic, MME can reproduce good mean state and monthly amplitude for SIE, but for SIV MME mean state and amplitude are smaller. In the Arctic, MME can reproduce good mean state and monthly amplitude for both SIE and SIV. CMIP5 simulations have very different variability (indicated by standard deviation of detrended monthly SIE and SIV) for different models. From Tables 1 and 2 we can conclude that the performance of each model is different. For the Antarctic, ACCESS1.0, BCC-CSM1.1, CESM1-CAM5-1-FV2, CMCC-CM, EC-EARTH, GISS-E2-H-CC, MIROC-ESM, MIROC-ESM-CHEM, MRI-CGCM3, MRI-ESM1 and NorESM1-M can give better SIE and SIV mean state. For the Arctic, ACCESS1.3, CCSM4, CESM1-BGC, CESM1-CAM5, CESM1-CAM5-1-FV2, CESM1-FASTCHEM, EC-EARTH, MIROC5, NorESM1-M and NorESM1-ME can give better mean state of SIE and SIV. The Arctic SIE linear trends of BNU-ESM, CanCM4, CESM1-FASTCHEM, EC-EARTH, GFDL-CM2p1, HadCM3, HadGEM2-AO, MIROC-ESM-CHEM, MPI-ESM-MR and MRI-ESM1 are closed to the observations.

Both satellite-observed Antarctic SIE and GIOMAS Antarctic SIV show increasing trends over the period of 1979-2005, but CMIP5 MME Antarctic SIE and SIV have decreasing trends. Only eight models' SIE and eight models' SIV show increasing trends. Can these few CMIP5 models give correct Antarctic sea ice trend? If we use these eight CMIP5 models to plot Antarctic SIC trends (not shown) as in Fig. 4, we will find that these eight CMIP5 model mean SIC trends have different spatial patterns with the observations (Fig. 3) although their model mean SIE and SIV have increasing trends. Satellite observed Antarctic SIE has increased trends, but when we use satellite observed sea ice record, we should also keep in mind that satellite observed sea ice record may also has large uncertainty. Eisenman et al. (2014) point out that sensor transition may cause a substantial change in the long-term trend.

We can see that the CMIP5 MME does a good job in terms of climatological mean, but their inter-model spread is large. The number of models used in published studies is usually less than the total CMIP5 models. How many models can give similar good simulations as all the available CMIP5 models? We first choose the CMIP5 models randomly. The model number changes from 1 to 49. We then calculate the SIE and SIV RMS errors between MME and observations or GIOMAS and PIOMAS datasets. For each fixed model number, we choose these models randomly many times, and then calculate the mean of the RMS errors. Figure 11 shows the ratio of SIE and SIV RMS errors between the errors calculated using different number of CMIP5 models and the errors calculated using all 49 CMIP5 models. We can see that the model errors decrease quickly as the model number increases; and the more models we use, the smaller error we have. For a fixed model number, the ratios of SIE are larger than the ratios of SIV, and Antarctic SIE has the largest ratio. When the model number is greater than 30, the model errors do not change much anymore. If we choose a criterion of RMS error larger than 15% of all the model RMS error, the model number of 22 is the critical number for Arctic SIE. It means that more than 22 CMIP5 models should give similar MME as all 49 CMIP5 models.

In this study, satellite observations, PIOMAS and GIOMAS data during the period of 1979-2005 are used to access the sea ice simulations from CMIP5 models. We always expect the models can capture the observed trends during this period. But we should note that simulations without data assimilation are always out of phase with the natural variability seen in the observations. So the differences between simulations and observations can either be due to model biases or natural climate variability (Stroeve et al., 2014).

Acknowledgments

Satellite-observed sea ice concentration data are provided by http://nsidc.org/data/seaice/, sea ice extent are from ftp://sidads.colorado.edu/DATASETS/NOAA/G02135/, GIOMAS sea ice date are downloaded from http://psc.apl.washington.edu/zhang/Global_seaice/index.html, and PIOMAS sea ice date are from http://psc.apl.washington.edu/wordpress/research/projects/arctic-sea-ice-volume-anomaly/. CMIP5 sea ice simulations are downloaded from http://pcmdi9.llnl.gov/esgf-web-fe/. The authors thank the above data providers. This work is supported by the National Basic Research Program of China (973 Program) under Grant 2010CB950500, National Natural Science Foundation of China (Grant Numbers. 41406027 and 41306206), the Project of Comprehensive Evaluation of Polar Areas on Global and Regional Climate Changes (CHINARE2014-04-04, CHINARE2014-04-01, and CHINARE2014-01-01), and Polar Strategic Research Foundation of China (20120103).

References

Cavalieri, D. J., Parkinson, C. L., Gloersen, P., and Zwally, H.: Sea Ice Concentrations from Nimbus-7 SMMR and DMSP SSM/I-SSMIS Passive Microwave Data, Boulder, Colorado USA: NASA DAAC at the National Snow and Ice Data Center, 1996.

Cavalieri, D. J., Gloersen, P., Parkinson, C. L., Comiso, J. C., and Zwally, H. J.: Observed hemispheric asymmetry in global sea ice changes, Science, 278(5340), 1104-1106, 1997.

Cavalieri, D. J., Parkinson, C. L., and Vinnikov, K. Y: 30-Year satellite record reveals contrasting Arctic and Antarctic decadal sea ice variability, Geophysical Research Letters, 30, 1970, doi:10.1029/2003GL018031, 2003.

Eisenman, I., Meier, W. N., and Norris, J. R.: A spurious jump in the satellite record: has Antarctic sea ice expansion been overestimated?, The Cryosphere, 8, 1289-1296, doi:10.5194/tc-8-1289-2014, 2014.

Kurtz, N., and Markus T.: Satellite observations of Antarctic sea ice thickness and volume, Journal of Geophysical Research, 117, doi:10.1029/2012JC008141, 2012.

Liu, J., Song, M., Horton, R. M., and Hu, Y.: Reducing spread in climate model projections of a September ice-free Arctic, Proceedings of the National Academy of Sciences, 110(31), 12571-12576 , 2013.

Mahlstein, I., Gent, P. R., and Solomon, S.: Historical Antarctic mean sea ice area, sea ice trends, and winds in CMIP5 simulations, Journal of Geophysical Research: Atmospheres, 118(11), 5105-5110, 2013.

Massonnet, F., Fichefet, T., Goosse, H., Bitz, C. M., Philippon-Berthier, G., Holland, M. M., and Barriat, P.-Y.: Constraining projections of summer Arctic sea ice, The Cryosphere, 6, 1383-1394, doi:10.5194/tc-6-1383-2012, 2012.

Polvani, L. M., and Smith, K. L.: Can natural variability explain observed Antarctic sea ice trends? New modeling evidence from CMIP5, Geophysical Research Letters, 40(12), 3195-3199, 2013.

Stroeve, J. C., Barrett, A., Serreze, M., and Schweiger, A.: Using records from submarine, aircraft and satellite to evaluate climate model simulations of Arctic sea ice thickness, The Cryosphere Discussions, 8, 2179–2212, 2014.

Stroeve, J. C., Kattsov, V., Barrett, A., Serreze, M., Pavlova, T., Holland, M., and Meier, W. N.: Trends in Arctic sea ice extent from CMIP5, CMIP3 and observations, Geophysical Research Letters, 39, L16502, doi:10.1029/2012GL052676, 2012.

Turner, J., Comiso, C., Marshall, G. J., Lachlan-Cope, T. A., Bracegirdle, T., Maksym, T., Meredith, M. P., Wang, Z., and Orr, A.: Non-annular atmospheric circulation change induced by stratospheric ozone depletion and its role in the recent increase of Antarctic sea ice extent, Geophysical Research Letters, 36, L08502, doi:10.1029/2009GL037524, 2009.

Turner, J., Bracegirdle, T. J., Phillips, T., Marshall, G. J., and Hosking, J. S.: An Initial Assessment of Antarctic Sea Ice Extent in the CMIP5 Models, Journal of Climate, 26, 1473–1484, doi: http://dx.doi.org/10.1175/JCLI-D-12-00068.1, 2013.

Vaughan, D. G., Marshall, G. J., Connolley, W. M., Parkinson, C., Mulvaney, R., Hodgson, D. A., King, J. C., Pudsey, C. J., and Turner, J.: Recent rapid regional climate warming on the Antarctic Peninsula, Climatic Change, 60(3), 243-274, 2003.

Worby, A. P., Geiger, C. A., Paget, M. J., Van Woert, M. L., Ackley, S. F., and DeLiberty, T. L.: Thickness distribution of Antarctic sea ice, Journal of Geophysical Research: Oceans, 113, C05S92, doi:10.1029/2007JC004254, 2008.

Xie, H., Tekeli, A. E., Ackley, S. F., Yi, D., and Zwally, H. J.: Sea ice thickness estimations from ICESat altimetry over the Bellingshausen and Amundsen Seas, 2003–2009, Journal of Geophysical Research: Oceans, 118(5), 2438-2453, 2013.

Zhang, J., and Rothrock, D.: Modeling global sea ice with a thickness and enthalpy distribution model in generalized curvilinear coordinates, Monthly Weather Review, 131 , 845–861, 2003.

Zunz, V., Goosse, H., and Massonnet, F.: How does internal variability influence the ability of CMIP5 models to reproduce the recent trend in Southern Ocean sea ice extent?, The Cryosphere, 7, 451-468, doi:10.5194/tc-7-451-2013, 2013.

Zwally, H. J., Comiso, J. C., Parkinson, C. L., Cavalieri, D. J., and Gloersen, P.: Variability of Antarctic sea ice 1979–1998, Journal of Geophysical Research: Oceans, 107(C5), 9-1-9-19, 2002.

Figures

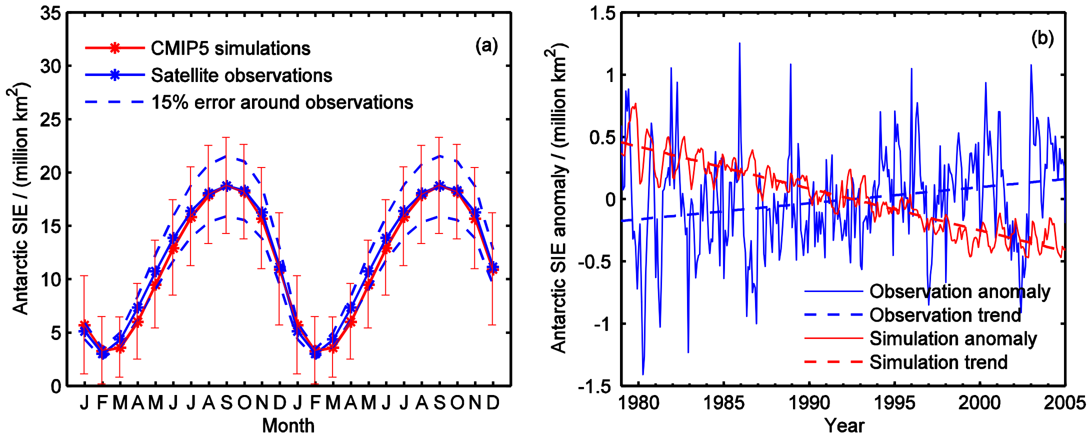

Figure 1. Climatology (a), anomaly and linear trend (b) of satellite observed and CMIP5 simulated Antarctic sea ice extent during 1979-2005. Two annual cycles are plotted in (a). The error bar is the range of one standard deviation.

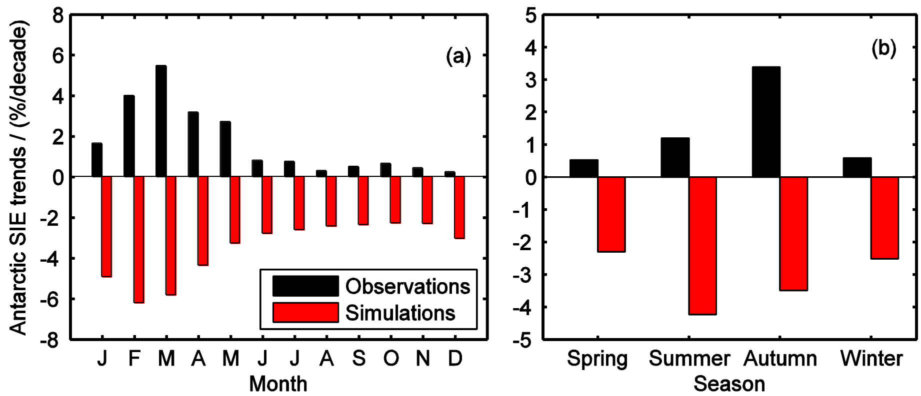

Figure 2. Monthly (a) and seasonal (b) linear trends of satellite observed and CMIP5-simulated Antarctic sea ice extent during 1979-2005.

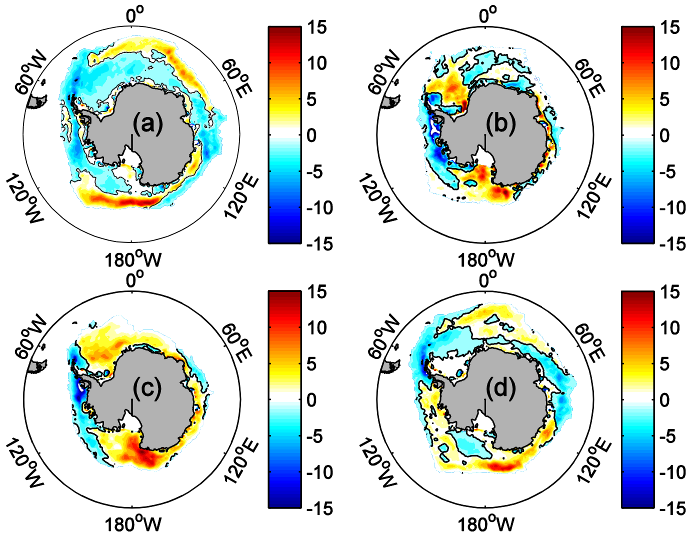

Figure 3. Linear trends (unit: % per decade) of satellite observed Antarctic sea ice concentration during 1979 to 2005. (a) Spring, (b) summer, (c) autumn, and (d) winter.

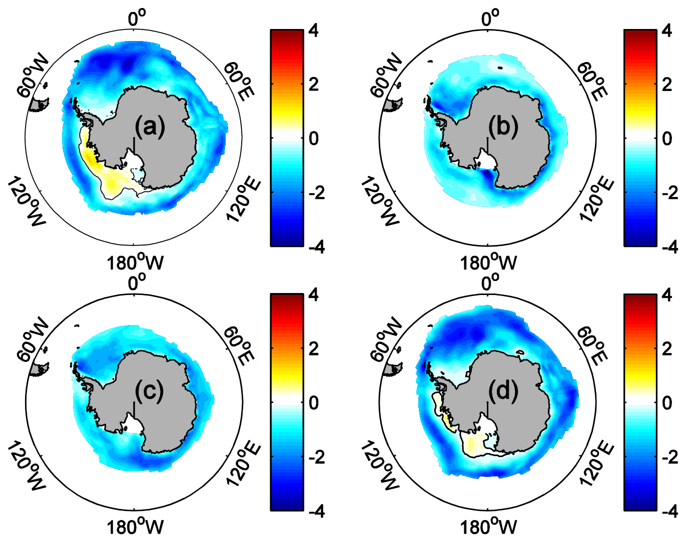

Figure 4. Linear trends (units: % per decade) of CMIP5-simulated Antarctic sea ice concentration during 1979-2005. (a) Spring, (b) summer, (c) autumn, and (d) winter.

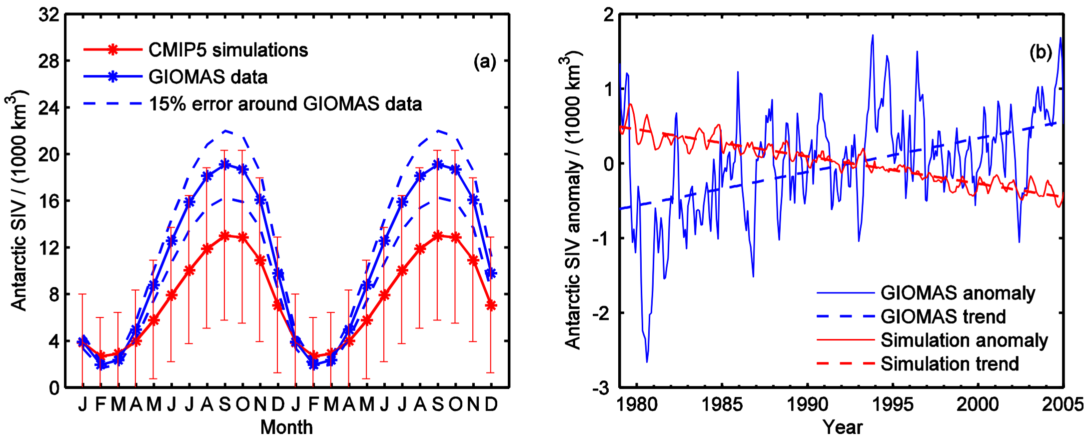

Figure 5. Climatology (a), anomaly and linear trend (b) of GIOMAS and CMIP5 simulated Antarctic sea ice volume during 1979-2005. Two annual cycles are plotted in (a). The error bar is the range of one standard deviation.

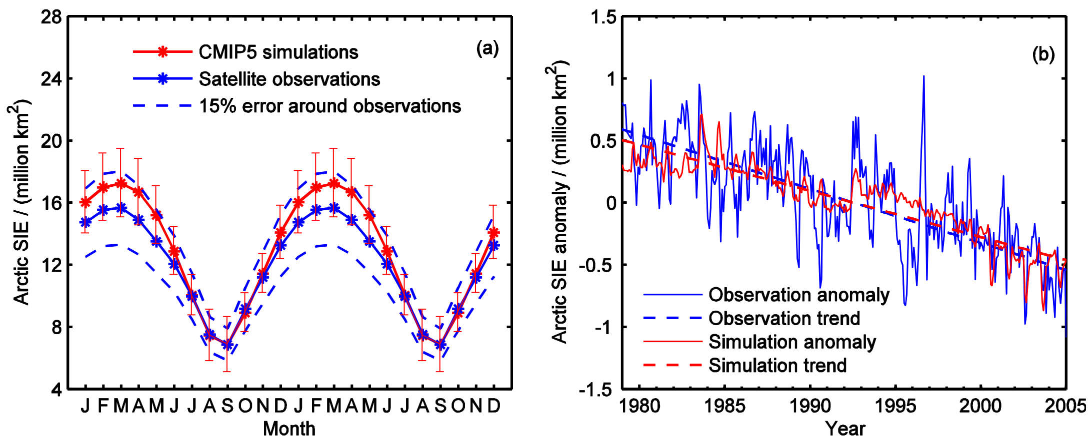

Figure 6. Climatology (a), anomaly and linear trend (b) of satellite observed and CMIP5-simulated Arctic sea ice extent during 1979-2005. Two annual cycles are plotted in (a). The error bar is the range of one standard deviation.

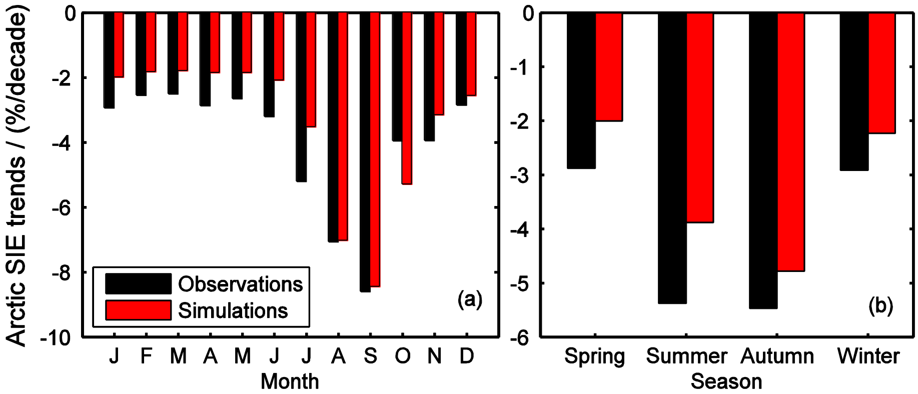

Figure 7. Monthly (a) and seasonal (b) linear trends of satellite observed and CMIP5-simulated Arctic sea ice extent during 1979-2005.

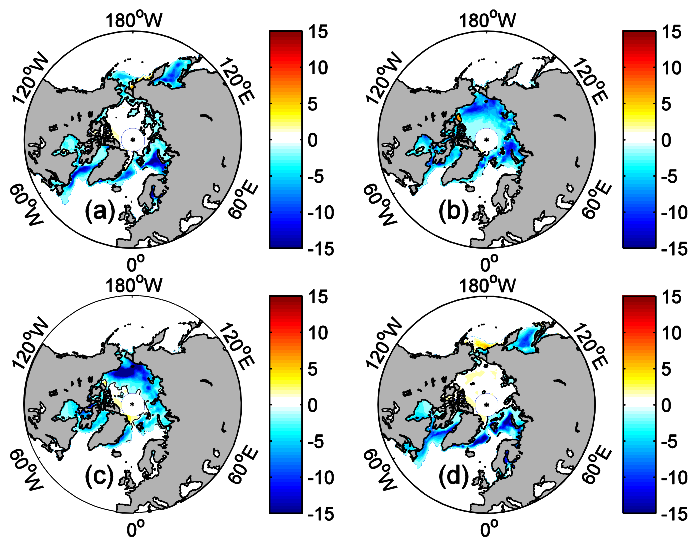

Figure 8. Linear trends (units: % per decade) of satellite observed Arctic sea ice concentration during 1979-2005. (a) Spring, (b) summer, (c) autumn, and (d) winter.

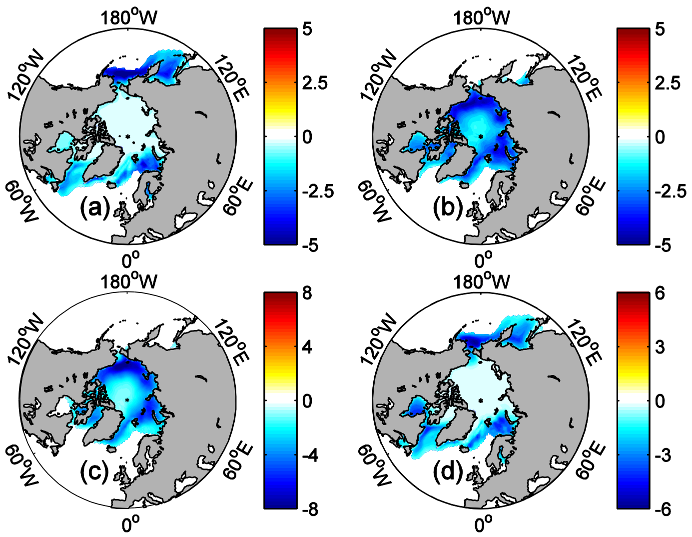

Figure 9. Linear trends (units: % per decade) of CMIP5-simulated Arctic sea ice concentration during 1979-2005. (a) Spring, (b) summer, (c) autumn, and (d) winter.

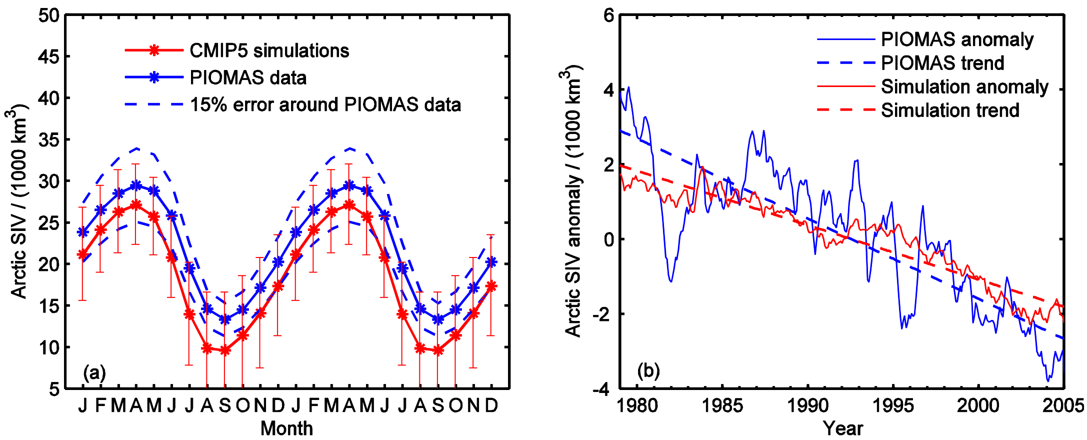

Figure 10. Climatology (a), anomaly and linear trend (b) of PIOMAS and CMIP5-simulated Arctic sea ice volume during 1979-2005. Two annual cycles are plotted in (a). The error bar is the range of one standard deviation.

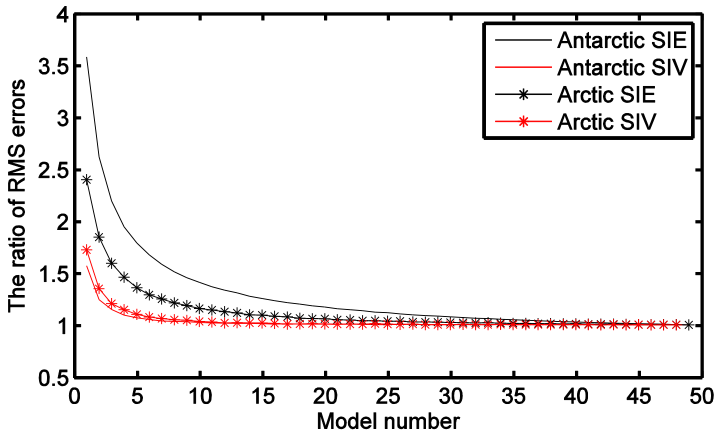

Figure 11. The ratio of SIE and SIV RMS errors between the errors calculated using different number of CMIP5 models and the error calculated using all 49 CMIP5 models.

Tables

Table 1. Antarctic sea ice metrics in CMIP5 models, satellite observations and GIOMAS dataset. Column (a) is mean annual SIE in million km^2. Column (b) is monthly SIE amplitude in million km^2. Column (c) is standard deviation of detrended monthly SIE anomaly in million km^2. Column (d) is linear trend in monthly SIE in 10^5 km^2 decade^{-1}, and the value in parentheses is 95% confidence level. Column (e) is monthly SIE root mean square error in million km^2. Column (f) is mean annual SIV in 10^3 km^3. Column (g) is monthly SIV amplitude in 10^3 km^3. Column (h) is standard deviation of detrended monthly SIV anomaly in 10^3 km^3. Column (i) is linear trend in monthly SIV in 10^3 km^3 decade^{-1}, and the value in parentheses is 95% confidence level. Column (j) is monthly SIV root mean square error in 10^3 km^3.

Data sources or CMIP5 models	(a)	(b)	(c)	(d)	(e)	(f)	(g)	(h)	(i)	(j)
Observations or GIOMAS	11.94	15.70	0.40	1.29(0.57)	----	11.02	17.17	0.63	0.45(0.09)	----
Multi-model ensemble mean (MME)	11.50	15.46	0.11	-3.36(0.15)	0.71	7.73	10.31	0.10	-0.36(0.01)	4.20
ACCESS1.0	12.10	19.12	0.59	-1.72(0.83)	1.57	6.30	11.35	0.43	-0.15(0.06)	5.20
ACCESS1.3	14.24	15.77	0.54	-0.97(0.77)	2.31	10.71	9.78	0.67	-0.03(0.09)	2.75
BCC-CSM1.1	13.42	19.32	**1.27**	**2.71(1.78)**	2.11	7.13	11.51	0.92	**0.09(0.13)**	4.41
BCC-CSM1-1-M	12.26	18.86	**1.06**	-20.03(1.49)	1.52	5.65	9.98	0.71	-1.20(0.10)	5.92
BNU-ESM	**20.60**	**23.46**	0.82	-9.60(1.15)	9.19	18.49	22.48	0.87	-2.03(0.12)	7.89
CanCM4	14.65	20.58	0.74	-2.79(1.03)	3.40	3.09	4.81	0.28	-0.06(0.04)	9.21
CanESM2	14.69	20.64	**0.96**	-7.74(1.35)	3.42	3.09	4.82	0.40	-0.15(0.06)	9.22

Data sources or CMIP5 models	(a)	(b)	(c)	(d)	(e)	(f)	(g)	(h)	(i)	(j)
CCSM4	18.37	13.70	0.58	-7.34(0.82)	6.64	19.34	18.63	1.12	-1.56(0.16)	8.34
CESM1-BGC	17.67	14.05	0.49	-6.68(0.69)	5.93	18.28	18.31	0.91	-1.19(0.13)	7.28
CESM1-CAM5	14.06	14.78	0.47	-5.52(0.66)	2.58	11.22	16.05	0.58	-0.97(0.08)	1.13
CESM1-CAM5-1-FV2	13.01	14.11	0.58	-3.16(0.82)	1.77	9.96	14.12	0.74	-0.22(0.10)	1.89
CESM1-FASTCHEM	17.86	13.42	0.60	-8.78(0.84)	6.14	18.41	18.15	1.18	-1.70(0.17)	7.42
CESM1-WACCM	14.33	12.57	0.39	-6.45(0.54)	2.95	11.55	13.15	0.66	-0.91(0.09)	1.80
CMCC-CESM	11.84	19.43	**0.99**	**2.91(1.39)**	2.01	6.70	11.18	0.71	**0.26(0.10)**	4.91
CMCC-CM	11.81	16.84	0.67	-2.49(0.94)	0.90	6.82	10.14	0.48	-0.05(0.07)	4.97
CMCC-CMS	11.74	19.33	0.87	-1.52(1.23)	1.83	6.31	10.70	0.59	-0.12(0.08)	5.34
CNRM-CM5	7.78	16.98	0.77	-2.59(1.09)	4.53	3.01	7.81	0.42	-0.10(0.06)	8.79
CNRM-CM5-2	9.28	14.08	**1.08**	**4.29(1.51)**	3.16	4.93	9.78	1.02	**0.38(0.14)**	6.77
CSIRO-Mk3.6	15.92	12.11	0.67	-1.64(0.95)	4.89	12.13	13.28	0.65	-0.29(0.09)	2.62
EC-EARTH	10.66	17.18	0.66	-7.94(0.92)	1.72	6.09	9.44	0.58	-0.66(0.08)	5.75
FGOALS-g2	17.10	17.29	0.48	-1.47(0.67)	5.28	15.65	13.89	0.74	-0.14(0.10)	4.88
FIO-ESM	17.19	12.21	0.49	-8.53(0.68)	5.61	21.23	13.98	1.16	-1.57(0.16)	10.31
GFDL-CM2p1	8.00	15.38	0.81	-6.33(1.14)	4.01	2.45	5.55	0.30	-0.19(0.04)	9.57
GFDL-CM3	6.25	12.06	0.73	-6.82(1.02)	5.82	1.92	4.16	0.37	-0.30(0.05)	10.29
GFDL-ESM2G	8.11	14.34	0.63	-4.45(0.88)	3.90	2.71	5.81	0.41	-0.24(0.06)	9.31
GFDL-ESM2M	6.39	12.23	0.41	-1.61(0.58)	5.65	1.81	4.20	0.16	-0.09(0.02)	10.36

Data sources or CMIP5 models	(a)	(b)	(c)	(d)	(e)	(f)	(g)	(h)	(i)	(j)
GISS-E2-H	6.21	10.62	0.38	-1.89(0.53)	6.03	3.24	7.19	0.27	-0.24(0.04)	8.65
GISS-E2-H-CC	12.18	19.07	0.75	-5.75(1.05)	1.52	6.70	14.16	0.51	-0.54(0.07)	4.57
GISS-E2-R	7.74	14.31	**1.01**	-3.39(1.42)	4.31	3.06	6.17	0.47	-0.16(0.07)	8.92
GISS-E2-R-CC	8.12	14.55	0.66	**0.82(0.92)**	3.93	3.12	6.24	0.35	0.00(0.05)	8.86
HadCM3	14.26	19.95	0.78	-2.74(1.10)	3.28	14.70	21.87	0.83	-0.49(0.12)	4.13
HadGEM2-AO	9.11	14.29	0.59	-5.31(0.83)	3.20	5.58	9.70	0.49	-0.42(0.07)	6.26
HadGEM2-CC	9.12	14.29	0.72	-0.85(1.02)	3.25	5.50	9.68	0.61	-0.05(0.09)	6.34
HadGEM2-ES	9.82	15.02	0.70	-3.25(0.98)	2.60	6.16	10.33	0.61	-0.41(0.09)	5.66
INMCM4	6.25	10.91	0.48	-4.00(0.68)	6.04	2.81	6.12	0.38	-0.28(0.05)	9.21
IPSL-CM5A-LR	9.66	19.06	0.84	-5.03(1.17)	3.43	4.13	8.66	0.53	-0.26(0.07)	7.70
IPSL-CM5A-MR	8.08	17.30	0.74	**1.69(1.04)**	4.56	2.80	6.50	0.35	**0.01(0.05)**	9.21
IPSL-CM5B-LR	3.34	8.09	0.42	**0.59(0.59)**	9.09	1.22	3.32	0.20	**0.04(0.03)**	11.10
MIROC4h	10.90	17.53	0.61	-7.96(0.86)	1.33	5.35	9.74	0.41	-0.51(0.06)	6.28
MIROC5	**3.23**	**6.62**	0.29	-1.03(0.41)	9.29	1.40	3.15	0.16	-0.07(0.02)	10.93
MIROC-ESM	12.65	19.12	0.64	-5.83(0.91)	1.47	7.23	10.72	0.47	-0.48(0.07)	4.46
MIROC-ESM-CHEM	13.38	19.80	0.53	-2.15(0.74)	2.07	8.08	11.59	0.49	-0.21(0.07)	3.61
MPI-ESM-LR	7.70	15.08	0.73	-2.95(1.03)	4.50	3.41	6.35	0.38	-0.19(0.05)	8.64
MPI-ESM-MR	7.90	15.62	0.84	**4.41(1.17)**	4.28	3.54	7.06	0.48	**0.24(0.07)**	8.39
MPI-ESM-P	7.91	15.69	0.75	-0.25(1.06)	4.34	3.48	6.48	0.45	**0.05(0.06)**	8.56

Data sources or CMIP5 models	(a)	(b)	(c)	(d)	(e)	(f)	(g)	(h)	(i)	(j)
MRI-CGCM3	13.43	15.99	0.66	**1.52(0.93)**	1.67	10.72	13.05	0.63	**0.22(0.09)**	2.04
MRI-ESM1	13.24	16.32	0.75	-0.62(1.05)	1.53	10.14	13.00	0.58	-0.03(0.08)	2.25
NorESM1-M	13.08	14.19	0.57	-0.71(0.80)	1.24	13.88	12.41	1.17	-0.07(0.16)	3.66
NorESM1-ME	16.98	14.19	0.60	-3.77(0.84)	5.24	17.57	16.82	1.40	-0.74(0.20)	6.59

Table 2. Arctic sea ice metrics in CMIP5 models, satellite observations and PIOMAS dataset. Column (a) is mean annual SIE in million km^2. Column (b) is monthly SIE amplitude in million km^2. Column (c) is standard deviation of detrended monthly SIE anomaly in million km^2. Column (d) is linear trend in monthly SIE in 10^5 km^2 $decade^{-1}$, and the value in parentheses is 95% confidence level. Column (e) is monthly SIE root mean square error in million km^2. Column (f) is mean annual SIV in 10^3 km^3. Column (g) is monthly SIV amplitude in 10^3 km^3. Column (h) is standard deviation of detrended monthly SIV anomaly in 10^3 km^3. Column (i) is linear trend in monthly SIV in 10^3 km^3 $decade^{-1}$, , and the value in parentheses is 95% confidence level. Column (j) is monthly SIV root mean square error in 10^3 km^3.

Data sources or CMIP5 models	(a)	(b)	(c)	(d)	(e)	(f)	(g)	(h)	(i)	(j)
Observations or PIOMAS	12.02	8.80	0.29	-4.35(0.41)	----	21.85	16.17	1.02	-2.14(0.14)	----
Multi-model ensemble mean (MME)	12.81	10.40	0.13	-3.71(0.19)	1.07	18.45	17.50	0.35	-1.45(0.05)	3.57
ACCESS1.0	12.13	10.33	0.41	-5.51(0.57)	0.94	15.41	18.74	1.05	-1.58(0.15)	6.60
ACCESS1.3	11.79	9.47	0.43	-0.78(0.60)	0.73	18.81	17.02	1.02	-1.05(0.14)	3.23

Data sources or CMIP5 models	(a)	(b)	(c)	(d)	(e)	(f)	(g)	(h)	(i)	(j)
BCC-CSM1.1	14.86	15.39	0.69	-8.79(0.97)	3.70	14.29	22.70	1.00	-2.01(0.14)	8.02
BCC-CSM1-1-M	13.19	15.96	0.65	-5.19(0.92)	2.87	11.04	20.69	0.87	-0.74(0.12)	11.02
BNU-ESM	14.72	12.61	0.50	-4.41(0.70)	3.19	23.03	19.79	1.23	-4.37(0.17)	1.83
CanCM4	12.79	14.77	0.52	-4.97(0.73)	2.49	11.41	15.35	0.97	-0.38(0.14)	10.47
CanESM2	12.01	13.76	0.49	-6.80(0.69)	1.91	**9.97**	14.21	0.63	-1.18(0.09)	11.92
CCSM4	12.33	8.56	0.44	-1.34(0.62)	0.42	20.27	16.16	1.51	-1.54(0.21)	1.82
CESM1-BGC	12.10	7.96	0.41	-2.85(0.58)	0.35	20.30	15.52	1.51	-2.63(0.21)	1.86
CESM1-CAM5	12.33	8.35	0.38	-1.87(0.53)	0.52	22.73	16.01	1.96	-1.22(0.28)	1.35
CESM1-CAM5-1-FV2	12.52	8.68	0.42	-5.07(0.59)	0.64	23.17	16.01	1.87	-3.63(0.26)	1.49
CESM1-FASTCHEM	12.02	8.86	0.39	-3.70(0.55)	0.25	18.27	15.86	1.37	-1.98(0.19)	3.69
CESM1-WACCM	13.44	8.10	0.36	-2.88(0.51)	1.51	27.32	9.47	2.07	0.09(0.29)	6.27
CMCC-CESM	13.97	9.33	0.36	-2.63(0.51)	2.12	28.75	11.93	1.38	-1.44(0.19)	7.11
CMCC-CM	13.99	7.35	0.30	-5.09(0.43)	2.06	**33.01**	9.87	1.73	-2.40(0.24)	11.52
CMCC-CMS	12.64	7.92	0.34	-2.87(0.48)	0.82	28.29	9.73	1.29	-1.18(0.18)	6.89
CNRM-CM5	12.41	11.41	0.46	-7.58(0.65)	1.11	14.44	20.22	0.99	-1.76(0.14)	7.60
CNRM-CM5-2	14.20	10.65	0.45	-2.32(0.63)	2.40	20.11	21.83	1.29	-0.96(0.18)	2.76
CSIRO-Mk3.6	**16.13**	7.57	0.30	-5.33(0.42)	4.20	25.94	12.16	0.81	-2.32(0.11)	4.30
EC-EARTH	12.45	8.04	0.35	-3.84(0.49)	0.57	24.01	12.44	1.90	-0.59(0.27)	2.86
FGOALS-g2	11.68	**3.35**	0.13	-1.44(0.18)	1.86	-----	----	----	----	----

Data sources or CMIP5 models	(a)	(b)	(c)	(d)	(e)	(f)	(g)	(h)	(i)	(j)
FIO-ESM	12.46	10.27	0.40	-2.23(0.57)	1.00	18.94	18.96	1.86	-1.69(0.26)	3.15
GFDL-CM2p1	12.58	12.85	0.54	-3.76(0.75)	1.68	11.11	18.13	0.87	-1.01(0.12)	10.80
GFDL-CM3	12.22	8.71	0.33	-2.89(0.46)	0.41	15.25	15.47	1.31	-1.18(0.18)	6.61
GFDL-ESM2G	**15.72**	13.72	0.48	-7.05(0.68)	4.24	16.91	19.33	1.24	-1.77(0.17)	5.17
GFDL-ESM2M	12.46	11.06	0.53	-0.31(0.74)	0.98	12.13	16.11	1.02	-0.56(0.14)	9.75
GISS-E2-H	12.96	14.87	0.54	-5.07(0.75)	2.47	13.61	25.67	0.76	-0.91(0.11)	9.10
GISS-E2-H-CC	13.94	14.24	0.60	-5.91(0.84)	2.80	14.94	27.49	0.80	-1.29(0.11)	8.23
GISS-E2-R	13.65	15.17	0.49	-6.31(0.69)	2.89	15.50	29.32	0.75	-1.28(0.11)	8.17
GISS-E2-R-CC	**15.13**	**16.73**	0.48	-5.65(0.67)	4.28	17.16	31.86	0.76	-1.08(0.11)	7.64
HadCM3	13.94	13.59	0.56	-4.74(0.78)	2.78	21.07	26.96	0.87	-2.25(0.12)	4.46
HadGEM2-AO	11.38	10.75	0.40	-3.81(0.56)	1.15	16.58	20.16	0.84	-0.98(0.12)	5.53
HadGEM2-CC	13.20	10.68	0.45	-3.10(0.63)	1.45	21.56	21.55	0.96	-2.47(0.13)	2.22
HadGEM2-ES	12.34	11.21	0.43	-6.03(0.60)	1.14	18.85	21.13	1.00	-1.69(0.14)	3.64
INMCM4	12.92	12.02	0.42	-0.21(0.59)	1.61	15.20	22.08	0.96	-0.21(0.13)	7.07
IPSL-CM5A-LR	12.72	10.07	0.44	-3.03(0.62)	1.14	21.87	16.41	1.48	-0.96(0.21)	1.66
IPSL-CM5A-MR	11.06	9.55	0.35	-2.85(0.49)	1.25	14.83	16.32	0.92	-1.69(0.13)	7.17
IPSL-CM5B-LR	14.06	8.28	0.40	-0.77(0.56)	2.08	27.28	13.11	2.91	-1.37(0.41)	6.25
MIROC4h	**10.66**	9.65	0.40	-3.11(0.56)	1.47	10.86	16.48	0.82	-1.00(0.12)	11.02
MIROC5	12.12	6.63	0.29	-6.78(0.40)	0.65	25.31	14.88	1.09	-3.68(0.15)	3.81

Data sources or CMIP5 models	(a)	(b)	(c)	(d)	(e)	(f)	(g)	(h)	(i)	(j)
MIROC-ESM	**10.40**	8.05	0.34	-1.91(0.47)	1.69	11.09	14.36	0.62	-1.04(0.09)	10.79
MIROC-ESM-CHEM	**10.83**	7.89	0.46	-4.24(0.65)	1.30	12.59	14.73	1.39	-1.69(0.20)	9.29
MPI-ESM-LR	11.10	7.95	0.40	-2.48(0.56)	1.01	15.07	16.87	0.85	-1.23(0.12)	6.85
MPI-ESM-MR	11.07	8.00	0.40	-4.94(0.56)	1.02	15.20	17.30	0.90	-1.75(0.13)	6.74
MPI-ESM-P	**10.94**	8.27	0.34	-1.83(0.48)	1.13	13.45	17.05	1.13	-0.80(0.16)	8.46
MRI-CGCM3	**15.01**	15.27	0.47	-1.44(0.66)	3.97	15.70	19.40	1.48	-0.55(0.21)	6.33
MRI-ESM1	14.65	14.67	0.61	-4.07(0.86)	3.52	15.21	18.89	1.74	-1.56(0.24)	6.76
NorESM1-M	12.01	5.96	0.25	-1.98(0.36)	0.90	23.77	11.23	1.57	-0.68(0.22)	3.11
NorESM1-ME	12.47	5.99	0.31	-0.21(0.43)	0.97	23.97	9.71	2.14	-0.46(0.30)	3.69

512